**Separation Science and Technology**
Publication details, including instructions for authors and subscription information:
http://www.informaworld.com/smpp/title~content=t713708471

# Analysis of a Thin Activated Carbon Loaded Adsorption Medium

Wayne T. Davis[a]; Christopher C. Hood[a]; Maureen Dever[b]
[a] Department of Civil and Environmental Engineering, University of Tennessee, Knoxville, Tennessee [b] Textiles and Nonwovens Development Center, University of Tennessee, Knoxville, Tennessee

**To cite this Article** Davis, Wayne T. , Hood, Christopher C. and Dever, Maureen(1995) 'Analysis of a Thin Activated Carbon Loaded Adsorption Medium', Separation Science and Technology, 30: 7, 1309 — 1324
**To link to this Article: DOI:** 10.1080/01496399508010348
**URL:** http://dx.doi.org/10.1080/01496399508010348

SEPARATION SCIENCE AND TECHNOLOGY, 30(7-9), pp. 1309-1324, 1995

# ANALYSIS OF A THIN ACTIVATED CARBON LOADED ADSORPTION MEDIUM

**Wayne T. Davis and Christopher C. Hood**
**Department of Civil and Environmental Engineering**
**University of Tennessee**
**Knoxville, Tennessee, 37996**
**and**
**Maureen Dever**
**Textiles and Nonwovens Development Center**
**University of Tennessee**
**Knoxville, Tennessee, 37996**

## ABSTRACT

Thin adsorption media are being investigated for use in a variety of applications including protective clothing for military use and hazardous waste cleanup, as well as in indoor air quality within a variety of filtration media. The objective of this study was to evaluate the dynamics of adsorption of a chlorinated organic gas on activated carbon impregnated meltblown laminates. The adsorption data were collected on a bench scale test stand on an existing battle dress overgarment and an experimental activated carbon impregnated liner material for use in protective clothing. Activated carbon loadings were nominally 40, 80, and 120 g/m$^2$. This paper reviews the results of the study and compares the experimental results to existing adsorption theory. For the organic compound, trichloroethylene, which was studied, a favorable isotherm was found. Although the materials were thin, the media provided a finite breakthrough, defined as a 1% penetration, followed by a gradual breakthrough curve similar to those typically observed in thicker bed adsorption systems.

Adsorption isotherms were developed for the activated carbon loaded laminates; the isotherms were of the Freundlich type. A conventional thick bed adsorption model was used to simulate and compare to the results obtained on the activated carbon loaded laminates. Unlike conventional activated carbon beds where the width of the breakthrough curve is a relatively small portion of the bed depth, the breakthrough curves for these thin laminates comprised a significant portion of the bed depth resulting in

breakthrough capacities which were substantially less than the overall absorption capacity of the laminates.

## APPROACH

### Description of Materials Tested

The approach used in this study was to prepare activated carbon impregnated laminates with nominal activated carbon loadings of 40, 80, and 120 g/m$^2$ by spraying a high surface area activated carbon (HSA) on to melt blown (MB) polyethylene (PE) webs. Laboratory testing revealed that the 33 g/m$^2$ PE MB webs with an average fiber diameter of 7.53 micrometers, thickness of .00004 m, and a permeability of 492 CFM/ft$^2$ were capable of retaining approximately 40 g/m$^2$ HSA carbon. Higher carbon loadings were obtained by layering the MB/PE webs. The activated carbon loaded webs were then sandwiched between two additional layers of MB/PE webs to prevent sloughing off of the activated carbon. Table 1 provides a detailed description of the laminates that were tested.

In addition to the prepared laminates, an existing material used as a battle dress overgarment (BDO) was also tested for comparison. The BDO consisted of a polyurathane foam nonwoven fabric impregnated with a slurry of latex binder and HSA activated carbon. The material was 0.0023 m (90 mils) thick with approximately 120 g/m$^2$ of HSA carbon, and an air permeability of approximately 50 cfm/ft$^2$. (1)

### Carbon Characteristics

The high surface area (HSA) activated carbon was manufactured by the Kansai Coke and Chemicals Company, Ltd (5 Misonocho, Amagaski City, Japan 660). The carbon had a surface area of 2,812 m$^2$/g and a pore volume of 0.776-0.855 cm$^3$/g. The activated carbon was applied to the surface of the pre-made MB media utilizing a fluidized bed spray and was entrained into the web. Since no adhesive was applied, the full benefit of the carbon's adsorptive capacity could be realized. The webs were weighed gravimetrically before and after application to determine the weight of HSA carbon retained. In general, samples were prepared in triplicate as shown in Table 1.

**TABLE 1. Characteristics of the Melt Blown and Spunbond Nonwovens**

| Laminate | Air Permeability CFM/ft$^2$ | Laminate Weight g/m$^2$ | Carbon Loading g/m$^2$ | Thickness m |
|---|---|---|---|---|
| Raw Laminate | | | | |
| Melt Blown | 492.2 | 33 | NA | 0.00004 |
| HSA Loaded Laminates | | | | |
| NG4-40 | 60.4 | 144 | 39 | 0.0017 |
| NG5-40 | 64.5 | 157 | 26 | 0.0012 |
| NG6-40 | 58.0 | 144 | 39 | 0.0015 |
| NG7-80 | 26.9 | 268 | 72 | 0.0023 |
| NG8-80 | 26.9 | 248 | 85 | 0.0014 |
| NG9-80 | 47.9 | 274 | 78 | 0.0017 |
| NG10-120 | 34.8 | 254 | 91 | 0.0020 |
| NG11-120 | 14.8 | 300 | 104 | 0.0021 |
| NG12-120 | 31.9 | 339 | 144 | 0.0021 |

NA = Not Applicable

## Description of the Filter Test Stand

A stainless steel laboratory filter test stand was constructed to allow the experimental determination of the breakthrough curves and adsorption capacities of the activated carbon loaded media as shown in Figure 1. The diameter of the laminate exposed to the flow was 0.114 m (4.5 inches) with a filter area of 0.0103 m$^2$. Nitrogen gas containing a certified concentration of the challenge gas (1,1,1-trichloroethylene) was delivered from a compressed gas tank through a two stage regulator and a rotameter to the filter holder at a flowrate of one liter per minute, creating a filtration velocity of 0.0016 m/s. From the flowmeter the gas passed through a T fitting with ball valves in each line. This allowed the operator to by-pass the filter holder before and after the dynamic adsorption test and route the gas directly to the challenge gas detector to measure the inlet concentration. A 20 L/m flowrate of make up air (0 ppm of TCE) was added to the 1

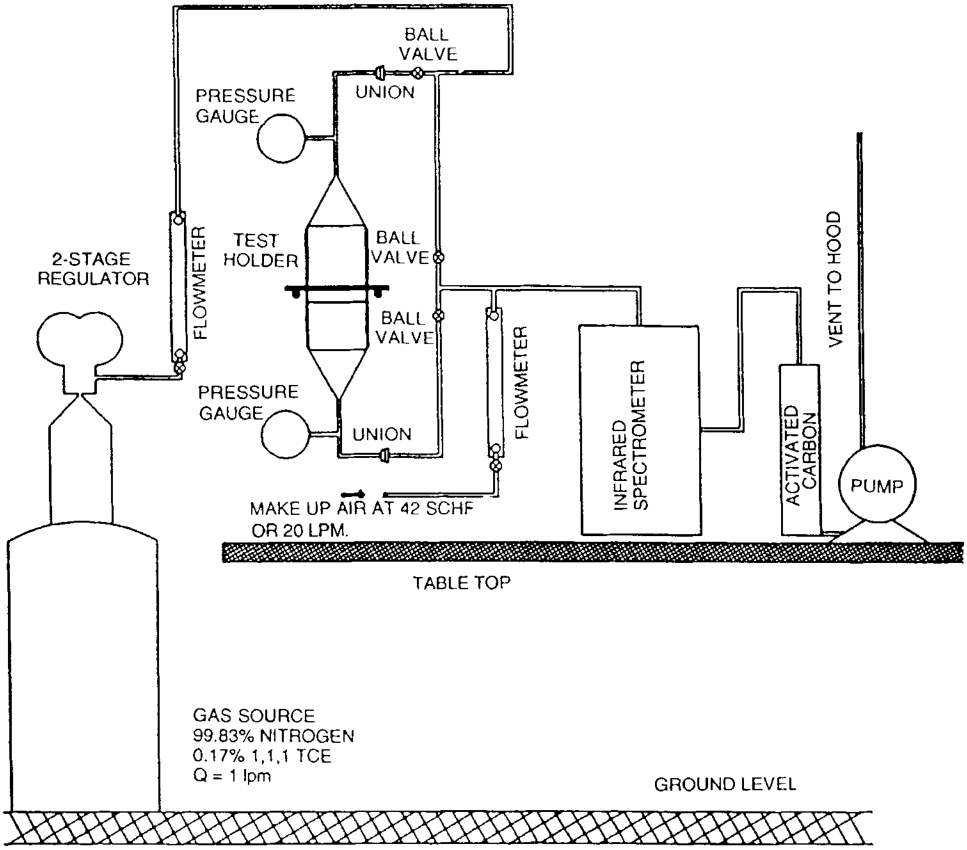

FIGURE 1. Schematic of bench scale adsorption test stand.

L/m flowrate leaving the test apparatus upstream of the detector to maintain a adequate response time in the detector. During the adsorption test, the gas was passed through the filter holder and then to the detector to measure the outlet concentration. The detector was a Miran 1A infrared spectrometer, with a minimum detectable concentration of 0.4 ppm, which was set up to continuously monitor the concentration of TCE. The flow then passed through a final activated carbon column to capture any challenge gas not adsorbed in the filter, and was exhausted into a laboratory exhaust hood.

Compressed gas cylinders of certified mixtures of TCE in nitrogen at concentrations of 174, 829, 1700, and 2125 ppmv of TCE were used in the study dependent on the objective.

## Description of Adsorption Tests

Two types of adsorption tests were conducted in the study. In the first set of tests, the objective was to determine the time required to reach breakthrough for the laminates at a fixed velocity of 0.0016 m/s at a TCE concentration of 1700 ppmv, and atmospheric pressure. To this extent, each laminate described in Table 1 was tested a minimum of two times. Prior to initial testing and between successive tests of the same laminate, the laminates were regenerated in a forced draft oven at 65°C for 24 hours to provide a base condition. The adsorption tests were conducted in the filter test stand and continuously monitored until an outlet TCE concentration of greater than one percent (17 ppmv) had been exceeded. The adsorption velocity of 0.0016 m/s was chosen in an attempt to simulate the velocity that might be created during the movement and flexing of protective clothing which might be worn. This is in contrast to the velocities normally found in thin beds of 0.125 m/s (2) and velocities found in thick industrial adsorption beds of 0.20-0.30 m/s (3).

In the second set of adsorption tests, a selected laminate (NG7-80), containing 72 g/m$^2$ of HSA carbon was tested at the above conditions until the total adsorption capacity had been reached using different TCE concentrations in an effort to establish the adsorption capacity of the carbon and to establish the adsorption isotherm for use in modeling.

## RESULTS

## Determination of Typical Breakthrough Curves

Figure 2 illustrates two typical breakthrough curves each for the BDO containing 120 g/m$^2$ of HSA carbon and the NG7-80 laminate which contained approximately 72 g/m$^2$ of HSA carbon using 1700 ppmv of TCE as described earlier. In both cases, the outlet concentration of TCE was initially below the detectable limit of 0.4 ppm. As time progressed, the TCE began to break through, reached the breakthrough point (1% or 17

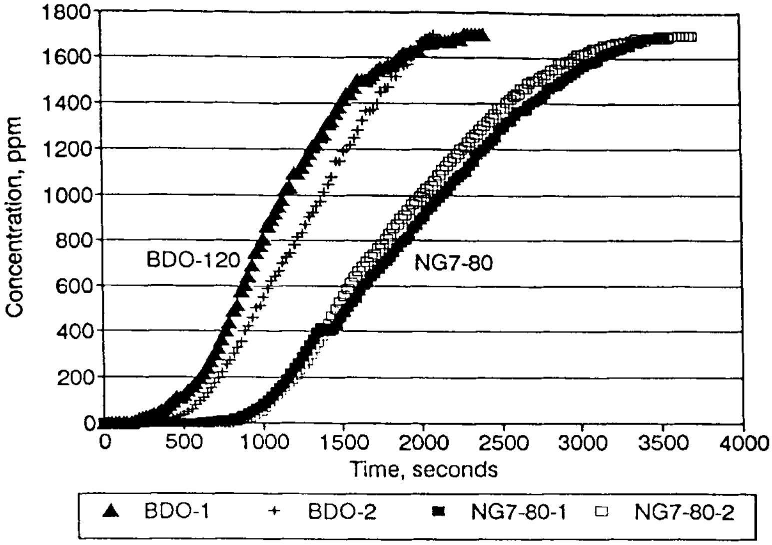

FIGURE 2. Comparison of BDO and MB/PE activated carbon laminates.

ppmv) and exhibited a classical breakthrough curve, eventually reaching the total adsorption capacity, at which time the outlet concentration reached 1700 ppmv. It is evident in Figure 2 that the MB/PE laminate had a greater capacity than the BDO even though it contained less HSA carbon. This is due to the fact that the BDO carbon was bound in the latex, whereas the MB/PE carbon was not bound, but simply adhering to the surface of the fibers. In a practical application, it would be necessary to bind the carbon particles to the fibers in some manner. Experiments to date have shown that binding by adhesives or by calendaring reduced the available carbon, thus reducing the time to breakthrough. (1)

## Effect of Carbon Loading on Breakthrough Time

Figure 3 provides an expanded view of Figure 2, illustrating the actual concentration profile of the two BDO and NG7-80 samples, illustrating the actual breakthrough point of 17 ppmv. An analysis was conducted of the breakthrough time for each of the prepared laminates. Figure 4 summarizes the breakthrough time versus the carbon loading for the laminates described in Table 1. Each filter was tested at least twice and

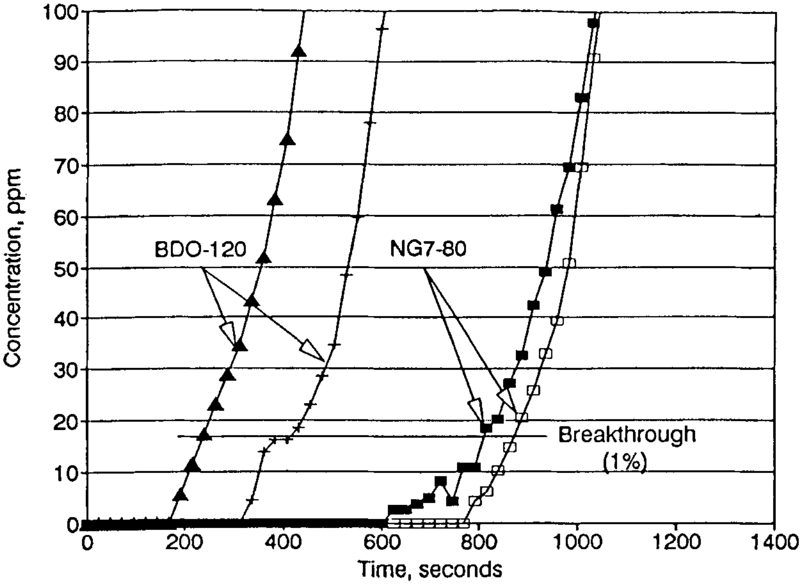

FIGURE 3. Behavior of breakthrough for BDO and MB/PE laminates.

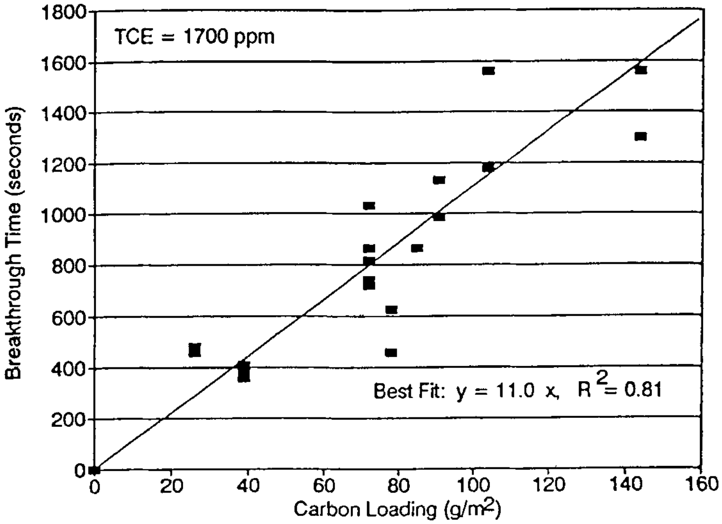

FIGURE 4. Breakthrough time versus activated carbon loading.

the breakthrough times were measured. As shown, there is an apparent linear relationship between the breakthrough time and the carbon loading. Scatter in the data is a combination of experimental error as well as the fact that the uniformity of the carbon distribution on the MB/PE laminates was variable due to the method of application. Based on this data, it can be concluded that while the media are thin, there is a finite and predictable breakthrough time which increases linearly with carbon loading. In this context, the adsorption data indicate that the media is not a "thin-bed" media, and may be modeled as a thick bed adsorption system.

## Development of Adsorption Isotherms

Both the breakthrough point and the saturation or equilibrium curves of adsorption systems have been documented to be a function of the concentration of the adsorbed gas, i.e., higher concentrations give rise to greater adsorption capacities. (4) In order to develop the actual equilibrium adsorption isotherm for the TCE adsorbed on HSA carbon, it was necessary to conduct a series of tests in which the adsorption tests were conducted to saturation or equilibrium capacity as shown in Figure 2. To this end, laminate NG7-80 with an HSA carbon loading of 72 $g/m^2$ was tested at TCE concentrations ranging from 174 to 2125 ppmv. Figure 5 illustrates the breakthrough curves for the four concentrations and shows that the higher concentrations break through earlier and reach saturation more quickly than the lower concentrations.

Figure 6 shows a graph of the adsorption isotherms for the laminates tested in this study. Curves are shown for the saturation or equilibrium adsorption capacity, which is the usual definition of the adsorption isotherm, as well as for the initial breakthrough capacity isotherm defined as a 1% penetration. For most thick bed systems, where the width of the breakthrough curve is extremely small compared to the depth of the bed the difference in the two isotherms is generally negligible. In the case of the thin media used in protective clothing, however, there is a significant difference in the equilibrium capacity and the initial breakthrough capacity. The equilibrium capacity ranged from less than 0.2 g of TCE/g of carbon at 174 ppmv to 0.4 g/g at 2125 ppmv. However, the 1% breakthrough capacity was less than .06 g/g at 174 ppmv and 0.2 g/g at 2125 ppmv, or approximately a 50-70% reduction in real operating capacity, dependent on the concentration.

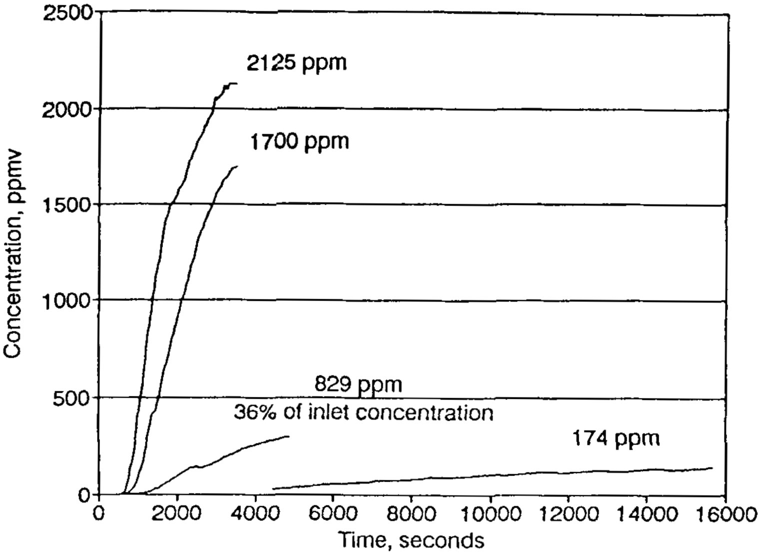

FIGURE 5. Breakthrough curves for four concentrations of TCE.

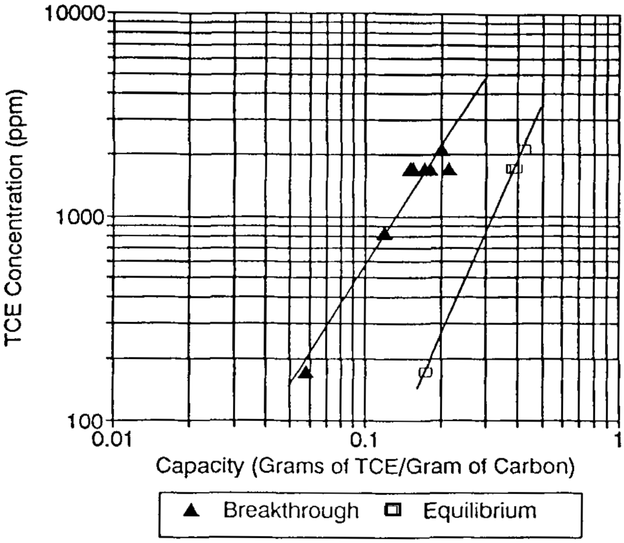

FIGURE 6. Adsorption Isotherms for breakthrough and equilibrium.

The data in Figure 6 also indicate that the adsorption isotherm is of the Freundlich type, exhibiting a linear curve on a log/log scale. The Freundlich isotherm as shown in Equation 1 is of the form used to develop an adsorption model which allows prediction of the behavior of the breakthrough curve. (4,5) The equation is as follows and represents the equilibrium concentration for both the gas and solid phase:

$$C_e = \alpha (X_{sat})^{\beta} \tag{1}$$

where:

$C_e$ = gas phase equilibrium concentration
$\alpha$ = experimental constant with concentration units
$\beta$ = constant based on experiment (unitless)
$X_{sat}$ = equilibrium mass adsorbed (g/g).

For the equilibrium data in Figure 6, the least squares fit equation for the Freundlich isotherm is as follows:

$$C_e = 24343 (X_{sat})^{2.81}$$

where $C_e$ is in ppmv of TCE, $\alpha$ is 24343 ppmv, and $\beta$ is 2.81 with an $R^2$ of 0.99. For $C_e$ in concentration units of kg/m$^3$ of TCE, $\alpha$ has a value of 0.1317 kg/m$^3$.

The equation for the 1% breakthrough capacity curve is:

$$C_{e,B} = \alpha_B (X_{sat,B})^{\beta_B}$$

where $C_{e,B}$ is the concentration in ppmv of TCE for the breakthrough capacity curve, $\alpha_B$ is 49021 ppmv, and $\beta_B$ is 1.93 with an $R^2$ of 0.93.

## APPLICATION OF MODELING OF ADSORPTION CURVES

### Review of Theoretical Equations

The development of the theoretical equations required to simulate the behavior of the adsorption wave as it propagates through an adsorption bed of thickness, L, is beyond the scope of this paper. A brief summary of this development is included herein to illustrate the principles. A complete detail of the development is provided by Wark and Warner (4), and Crawford (5). Figure 7 illustrates the concept of an adsorption wave

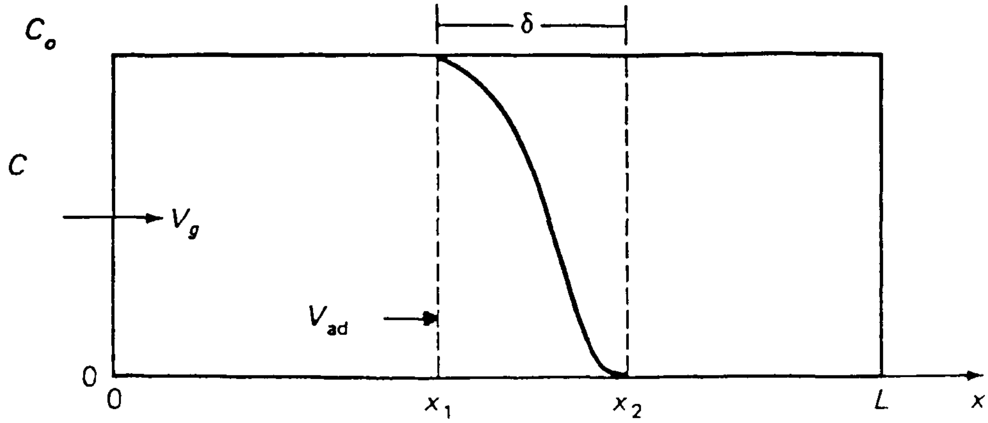

FIGURE 7. Theoretical adsorption wave.

of thickness, $\delta$, moving through a bed of thickness, L, at an adsorption wave velocity, $V_{ad}$. The superficial gas velocity approaching the bed is designated as $V_g$, and the inlet concentration is $C_o$. In the diagram, $x_1$ is the distance from the inlet of the bed to the back edge of the adsorption zone, usually defined as the location where $C = .99\ C_o$; x is the distance to the point at which the concentration has a value of C lying between 0.99 and .01 $C_o$; and $x_2$ is the front edge of the adsorption wave, usually defined as $C = .01\ C_o$. The equation for the adsorption wave velocity is:

$$V_{ad} = \frac{V_g}{\rho_{ad}} (\alpha)^{1/\beta} (C_o)^{(\beta-1)/\beta} \qquad (2)$$

where $\rho_{ad}$ is the bulk density of the activated carbon in the bed. The adsorption wave velocity is important since it describes the movement of the adsorbate through the adsorbent. That information is used in turn to define the thickness of the mass transfer zone and the time to breakthrough for a given adsorber thickness.

Equation 3 describes the position in the adsorption zone and is dependent on the concentration limits. For this application of the model, the limits were set at 1 percent to 99 percent of the inlet concentration. The equation is as follows:

$$x = x_1 + \frac{V_g}{K}\left[\ln 0.99\frac{C_o}{C} + \frac{1}{\beta-1}\ln\frac{1-(C/C_o)^{\beta-1}}{1-(0.99)^{\beta-1}}\right] \qquad (3)$$

where K is a film resistance coefficient (units = time$^{-1}$).

These limits can be adjusted by replacing the 0.99 values in Equation 3 with the desired fraction of the inlet concentration value. It is important to remember that the curve is assumed to be symmetrical therefore the limits must be consistent with that symmetry.

Equations 1 - 3 are useful in providing a dynamic description of an adsorption system. However, when one is designing a system the time to breakthrough is the most important criteria. Equation 4 defines the breakthrough time, $t_b$:

$$t_b = \frac{L - \delta}{V_{ad}} \qquad (4)$$

In this equation one recognizes the importance of the velocity of the adsorption wave and width of the mass transfer zone. The value of delta, the width of the adsorption wave, can be evaluated by determining the value of $x - x_1$ for $C_0$ and C equal to 0.99 and .01, respectively in Equation 3.

## Modeling Results

By varying the value of C in Equation 3 from .99 to .01, it is possible to create the profile of the adsorption wave. By converting the distance to an equivalent point in time, one can then create a graph of the outlet concentration versus time similar to those shown in Figures 2, 3, and 5. A basic computer program was developed based on Equations 1-3 to predict the concentration at the outlet of the activated carbon impregnated laminates as a function of time. This predicted curve was then compared to the actual concentration versus time curves such as the one illustrated in Figure 2. It was necessary to shift the predicted outlet concentration curve to compensate for the fact that the above theory assumes that the adsorption wave is fully developed at the beginning of the bed and to ensure that the total area above the predicted concentration versus time curve actually yielded the total adsorption capacity predicted by the equation for the adsorption isotherm. This correction would have been insignificant in thick beds where the width of the adsorption wave is small compared to the overall bed depth, L.

Inputs to the calculation of the concentration versus time curve at the outlet of the adsorption filter for the data shown in Figure 2 for the NG7-80 laminate were:

Equation 1: $\alpha = 0.1317\ \text{kg/m}^3$
$\beta = 2.81$

Equation 2: $V_g = 0.00162\ \text{m/s}$
$\rho_{ad} = 31.3\ \text{kg/m}^3$
$C_o = 0.0092\ \text{kg/m}^3$ (1700 ppmv).

The value of K, the film resistance coefficient, for thin laminated materials where the density of the carbon is very small, and the velocity of the gas is very low were not available from the literature. An equation developed by Wheeler (6) and modified by Jonas et.al. (7), showed that the film resistance coefficient could be approximated by the equation:

$$K = \frac{657.6\ V_g^{0.5}}{M_w^{0.5}} \qquad (5)$$

where K has units of $\text{sec}^{-1}$, and $M_w$ is the molecular weight in g/mole of the gas being adsorbed.

In that study, the tests were conducted using carbon tetrachloride and several other organic gases, both chlorinated and non-chlorinated, using a 6-10 mesh activated carbon, at a velocity of 0.054 m/s. In addition, Wheeler (6) showed that the value of K was proportional to the diameter of the activated carbon granules to the minus 1.5 power, i.e. $d_p^{-1.5}$. Since the exact diameter of the granules in the study by Jonas were unknown, the coefficient in Equation 5 is specific to the carbon used in that study. Since specific information on the size of the granules was also unavailable in the current study, it was decided to use the above equation to provide an approximate estimate of the value of K for the tests conducted herein to conduct preliminary modeling. Based on the velocity of 0.00162 m/s in this study and the molecular weight of 1,1,1-trichlorethylene of 133.4 g/mole, the estimate of K using Equation 5 was 2.29 $\text{sec}^{-1}$. In actuality the value of K should be higher than this value, since the activated carbon used in the present study was a powdered high surface area carbon with a finer mesh size than 6-10 mesh.

Figure 8 provides a comparison between the experimental data collected on the NG7-80 laminate and the predicted breakthrough curve using Equations 1-5. The value of K was varied from 3 to 13.3 $\text{sec}^{-1}$ to provide an indication of its effect on the shape of the

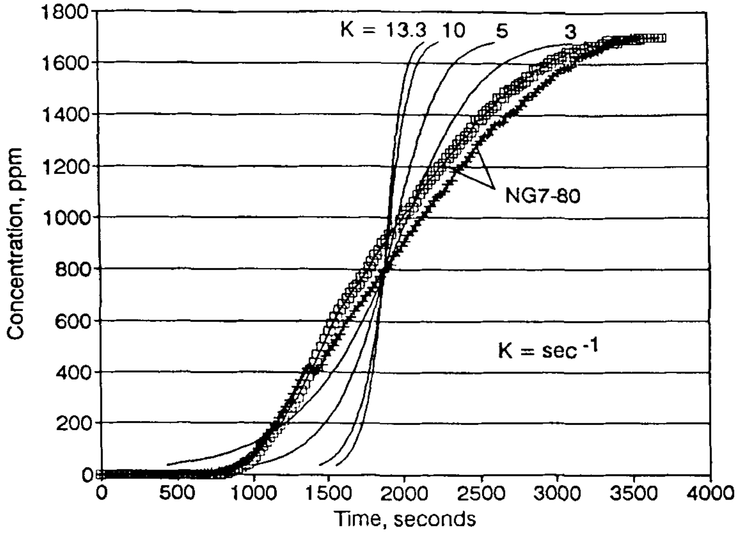

FIGURE 8. Comparison of observed and predicted breakthrough curves.

predicted breakthrough curve. As shown in the figure, and as predicted by the equations, a large value of K creates a very sharp or steep breakthrough curve. As the value of K is lowered, the curve has a lesser slope and results in an earlier breakthrough time. Based on the preliminary comparison of the equations to the experimental laminate data, it is apparent that the HSA activated carbon laminates have a K value that is in the range of those predicted by Equation 5. However, a K value of 3 sec$^{-1}$ created an earlier 1% breakthrough than was actually observed.

Since the K value is dependent on the type and size of carbon, an effort was made to experimentally determine a K value which would be more representative of the thin laminates with the HSA carbon. Equations 1-5 were used to predict the actual 1% breakthrough times shown in Figure 4 for all of the laminates tested. A statistical analysis was then conducted to determine the value of K which provided the highest correlation between the measured 1% breakthrough times shown in Figure 4 and the values predicted using Equations 1-5. The analysis revealed that a K value of 5.6 provided the highest correlation between the predicted and observed breakthrough times with an $R^2$ of 0.73. The comparison is shown in Figure 9. It is anticipated that the K

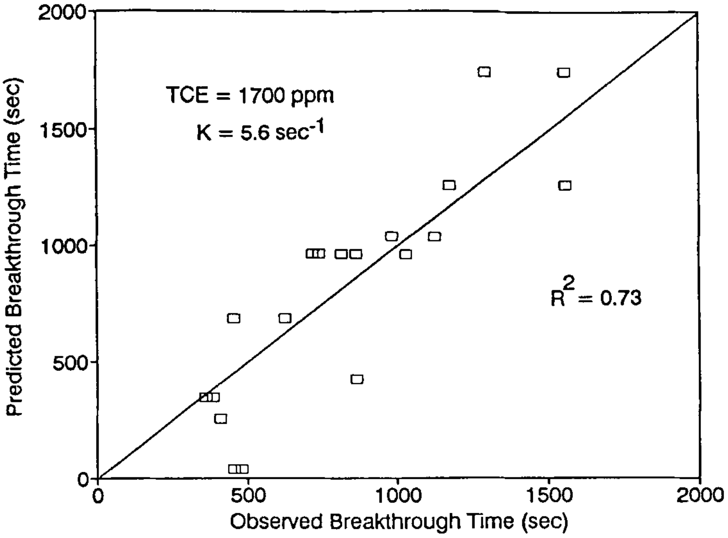

FIGURE 9. Comnparison of model predicted and observed breakthrough times.

value would also be a function of the molecular weight of the gas and the velocity in a manner similar to that shown in Equation 5. It may also be a function of the density of the activated carbon bed as well as the bed depth.

Placing the above empirically determined K value into the format used by Jonas in Equation 5 to account for velocity and molecular weight, it is recommended that the following equation be used to provide an estimate of the K value for other velocities and molecular weights using the HSA carbon:

$$K = \frac{1607\ V_g^{0.5}}{M_w^{0.5}} \qquad (6)$$

Additional testing is needed to confirm the sensitivity of K to other parameters, particularly in these thin laminates which have very low activated carbon densities due the random dispersion of the carbon within the laminate.

## CONCLUSIONS

Testing has shown that thin activated carbon impregnated melt blown laminates can be used to successfully adsorb organic gases under low velocity conditions similar to those used in protective clothing applications. The behavior of the laminates is similar to that of the more standard thicker bed activated carbon systems in that the laminates exhibited a classical breakthrough curve. In addition, it was possible to develop both breakthrough and equilibrium capacity adsorption isotherms; these were found to be of the Freundlich type. In contrast to the thicker bed systems, however, the "working" capacity, defined herein as a 1% breakthrough, was only about 50% of the equilibrium capacity, due to the fact that the width of the absorption wave comprised a relatively large fraction of the total depth of the filter.

Preliminary modeling based on knowledge of the adsorption isotherms and conventional equations describing the adsorption wave velocity and the shape of the adsorption wave, has shown that the adsorption characteristics of the laminates can be described. The film resistance coefficient, K, was found to be approximately 5.6 $\mathrm{sec}^{-1}$ for the thin laminates operated at low velocities with TCE as the adsorbate.

## REFERENCES

1. M. Dever, W.T. Davis, and C.C. Hood, "Development of an Activated Carbon Loaded Melt Blown-Spunbond Laminate," TAPPI JOURNAL, Vol. 77, No.2, February, 1994.

2. A. Turk, "Adsorption," in Air Pollution, 3rd Ed., Academic Press, New York, NY, pp. 329-363, 1977.

3. R.E. Treybal, Mass Transfer Operations, 2nd Ed., McGraw Hill Book Co., New York, NY, pp. 495-544, 1968.

4. K. Wark, and C. Warner, Air Pollution: Its Origin and Control, Harper Collins College Publishers, Glenview, IL, pp. 261-273, 1981.

5. M. Crawford, Air Pollution Control Theory, McGraw Hill, Inc., New York, NY, pp. 513-518, 1976.

6. A. Wheeler, and A. Robell, J. Cat., 13, 299, 1969.

7. L.A. Jonas, Y.B. Tewari, and E.B. Sansone, "Prediction of Adsorption Rate constants of Activated Carbon for Various Vapors," Carbon, Vol 17, pp. 345-349, 1979.